Changes in MM-CK Conformational Mobility upon Formation of the ADP−Mg^{2+}−NO_3^-−Creatine Transition State Analogue Complex As Detected by Hydrogen/Deuterium Exchange

Hortense Mazon,[‡] Olivier Marcillat,[‡] Eric Forest,[§] and Christian Vial*[,‡]

UMR CNRS 5013, Biomembranes et enzymes associés, Université Claude Bernard Lyon 1, 43, boulevard du 11 Novembre 1918, 69622 Villeurbanne cedex, France, and Laboratoire de spectrométrie de masse des protéines, Institut de Biologie Structurale, CNRS (UMR 5075)/CEA/UJF, 41 Avenue des Martyrs, 38027 Grenoble Cedex, France

Received July 9, 2003; Revised Manuscript Received September 2, 2003

ABSTRACT: In the presence of ADP, Mg^{2+}, creatine, and the planar nitrate ion, creatine kinase isoenzymes undergo significant structural changes accompanying the formation of a very stable transition state analogue complex (TSAC). We have compared, by using hydrogen/deuterium exchange followed by proteolysis of the labeled enzyme and mass spectrometric analysis of the peptic peptides, the backbone dynamics fluctuations of the free enzyme and those of the TSAC. In most peptides, exchange is not affected by ligand binding, except that observed in seven areas located in or at the entrance to the active site, where some protection is detected. On the basis of a comparison with the three-dimensional structures of free or liganded guanidino kinases, four of these peptides (residues 54−72, 226−234, 287−311, and 315−333) can be considered part of the substrate binding site. The other three (residues 162−186, 193−201, and 202−224) are not directly involved in the binding of substrates and are located in a dynamic domain, which allows the enzyme to properly align the substrates for optimal catalysis.

Creatine kinases (CKs) catalyze the reversible transfer of a phosphoryl group from $MgATP^{2-}$ to creatine, generating phosphocreatine and $MgADP^-$ in the cells of excitable tissues (for a review, see ref *1*). Creatine kinase isoenzymes are members of the large family of phosphagen kinases. In accordance with their important level of sequence similarity (∼60% identical across all species), all the reported structures of CKs are highly homologous. After numerous unsuccessful trials, the first CK isoenzyme for which an X-ray structure has been determined is mitochondrial CK from chicken heart (*2*, *3*). The structures of several other creatine kinase isoenzymes have now been determined. These include rabbit muscle MM-CK[1] (*4*), chicken BB-CK (*5*), human ubiquitous mitochondrial CK (*6*), and human MM-CK (*7*).

Monomers in the dimeric MM enzyme (PDB entry 2crk) display a two-domain organization with a small N-terminal domain (∼100 residues) containing only helical structure elements and a large C-terminal domain (residues 120−380) consisting of an eight-stranded antiparallel β-sheet surrounded by seven α-helices (*4*). The substrate binding site is located between these two domains. Sequence alignment of the CK isoenzymes reveals six highly conserved regions which form a compact core involved in substrate binding and catalysis (*2*). Several monomer−monomer contact areas allow for the formation of a stable dimer (*4*, *8*).

Conformational changes induced by substrate binding to creatine kinase, as well as other phosphagen kinases, have been known for a long time. For instance, the binding of magnesium complexes of ADP and ATP, but not of creatine alone, produces specific shifts in the absorption spectra of CK (*9*, *10*). It has also long been known that the CK intrinsic fluorescence is quenched upon ADP binding (*11*−*13*), and the quenchable residue was later shown to be the conserved tryptophan 227 (*14*, *15*). These results reflect alterations of the environment of aromatic residues upon substrate binding.

In the presence of ADP, Mg^{2+}, nitrate, and creatine, the various CK isoenzymes form a dead-end inhibition complex. This complex is an analogue of the transition state of the enzymatic reaction in which the anion occupies the position of the transferable phosphate of ATP (*16*). Two structures of the transition state analogue complex (TSAC) of phosphagen kinases have been described: that of arginine kinase (*17*) and very recently that of *Torpedo californica* CK (*18*). The active site is lined by two flexible loops, an N-terminal loop around residues 59−69 which is shorter in arginine kinase (*19*), and a C-terminal loop around residues 320−330. Substrate binding is accompanied by a movement of the two domains and a closing of the active site by these two loops.

* To whom correspondence should be addressed: UMR 5013 CNRS, Université Claude Bernard Lyon I, 43 boulevard du 11 Novembre 1918, 69622 Villeurbanne cedex, France. Telephone: 00 33 472 448 248. Fax: 00 33 472 431 557. E-mail: christian.vial@univ-lyon1.fr.

[‡] Université Claude Bernard Lyon 1.

[§] CNRS (UMR 5075)/CEA/UJF.

[1] Abbreviations: BB-CK, cytosolic dimeric creatine kinase BB; H/D, hydrogen/deuterium; DTT, dithiothreitol; LC/MS, liquid chromatography and mass spectrometry; MM-CK, cytosolic dimeric creatine kinase MM; MS/MS, tandem mass spectrometry; NH, amide hydrogen; TFA, trifluoroacetic acid; TSAC, transition state analogue complex.

10.1021/bi035208m CCC: $25.00
Published on Web 10/31/2003

Using electron paramagnetic resonance and proton relaxation rates, distinct structural changes have been recorded upon fixation of manganous complexes of nucleotides, and subsequent additions of creatine and nitrate anions (*20*), showing that the coordination sphere of the metal ion becomes much less accessible to solvent water.

The conformational changes occurring upon substrate binding and formation of the TSAC have been further documented. It has been shown that ADPMg protected CK from proteolysis and inactivation by proteinase K by ~50%. This level of protection increased to nearly 100% upon subsequent addition of creatine and NO_3^- (*21*). Furthermore, the cleavage by proteinase K at only one site of the enzyme destroys its ability to form a transition state analogue complex in the presence of Mg^{2+}, NO_3^-, ADP, and creatine (*22*). This effect was observed in all CK isoenzymes and was attributed to a cleavage in an exposed area near the C-terminal end (*23*, *24*). The exact position of the cleavage was determined (*25*) and later shown to be in a very mobile loop, the crystallographic structure of which cannot be resolved (*2*, *4*).

Addition of the nucleotide substrates has been shown to slow substantially the reaction of thiol reagents, such as DTNB or iodoacetate, with the active site Cys residue of CK, the maximum effect being attained with the TSAC (*26*). It has also been shown to modify the p*K* of histidines (*27*), the intrinsic fluorescence of the protein (*13*), and the exposition of tyrosyl residues (*28*). The presence of MgADP or MgATP protects against the inactivation due to Arg residue specific reagents (*29*).

The conformational changes that occur when substrates bind to cytoplasmic or mitochondrial isoenzymes of rabbit CK have also been studied in our laboratory using caged nucleotides and Fourier transform infrared spectroscopy (*30*−*32*). We have shown that binding of ADP, ATP, P_i, and the TSAC induced specific changes in the infrared spectrum, some of which could be assigned to groups of the peptide backbone.

At a more global level, small-angle X-ray scattering experiments demonstrated a reduction of the radius of gyration of CK from 28 Å (free enzyme) to 25.6 Å and from 28 Å (free enzyme) to 25.5 Å for the CK−ATP−Mg^{2+} complex and the CK−ADPMg−NO_3^-−creatine complex, respectively. A similar reduction was found for the mitochondrial enzyme. Addition of creatine or free nucleotides did not lead to any significant change (*33*).

Protein hydrogen exchange has became a powerful tool in analyzing the structure and dynamics of the proteins (*34*). For small soluble proteins, high-resolution NMR methods can measure hydrogen/deuterium (H/D) exchange rates (*35*). Mass spectrometry has allowed amide hydrogen exchange studies of larger proteins. The rates at which specific amide hydrogens exchange appear to depend on their solvent accessibility and their implication in the formation of specific hydrogen bonds. Mass spectrometry allows studies of the intact protein and, when combined with proteolysis and peptide mapping with MS/MS, the segment specific identification of solvent accessible exchange sites (*36*). Amide H/D exchange and mass spectrometry were successfully used to study the structural changes of proteins induced by the binding of substrates. For example, NADH binding to *Escherichia coli* dihydropicolinate reductase and that of NADPH and diaminopimelate to *Corynebacterium glutamicum* diaminopimelate deshydrogenase were studied by Wang *et al*. (*37*, *38*). The conformational changes of protein tyrosine phosphatase induced by vanadate, a competitive inhibitor, were investigated by the same group (*39*). Halgand *et al*. (*40*) analyzed the binding of Mg^{2+} and NADPH that lead to structural changes of acetohydroxy acid isomeroreductase. Andersen *et al*. (*41*) studied the binding of ADP to protein kinase A. This technique was also used to compare the stability of an enzyme and its active mutants (*42*). The aim of this work is to identify, using these techniques, the protein segments which are influenced by the formation of a TSAC in rabbit muscle MM-CK.

MATERIALS AND METHODS

Protein Preparation. Creatine kinase from rabbit muscle (MM-CK) was purchased from Roche. The enzyme was desalted by using a PD10 Sephadex G25 column (Pharmacia) equilibrated in 50 mM Tris-HCl buffer (pH 7). The protein concentration was estimated using a molar extinction coefficient of 76 000 M^{-1} cm^{-1} at 280 nm for MM-CK.

Materials. D_2O (99.9%) and chloroacetic acid (99%) were purchased from Aldrich, and creatine, TFA, DTT, and pepsin were from Sigma. Tris was purchased from Interchim, ADP from Amresco, $MgAc_2$ from Carlo Erba, and acetonitrile from SDS.

Hydrogen Exchange. Hydrogen exchange experiments were performed on the free enzyme or on the transition state analogue complex. For the TSAC, MM-CK in 50 mM Tris-HCl/H_2O buffer (pH 7) was diluted (1:1, v/v) into 50 mM Tris-HCl/H_2O buffer (pH 7) containing 5 mM DTT, 60 mM creatine, 20 mM $MgAc_2$, 50 mM $NaNO_3$, and 4 mM ADP for 2 min at 20 °C. Deuterium exchange was initiated by a 20-fold dilution of the enzyme with 50 mM Tris-DCl/D_2O buffer (pD 7) containing 30 mM creatine, 10 mM $MgAc_2$, 25 mM $NaNO_3$, and 2 mM ADP at 20 °C. The deuterated labeling solution was prepared by concentration to $^1/_5$ of its initial volume using a vacuum concentrator (SpeedVac). The concentrated solution was reconstituted with D_2O and then concentrated again. This step was repeated three times. For the free CK, the same protocol was used, but the buffers were 50 mM Tris-HCl/H_2O buffer (pH 7) containing 5 mM DTT and 50 mM Tris-DCl/D_2O buffer (pD 7). All pD measurements are given as the values read from the pHmeter with no adjustment for isotope effects (*43*). Isotope exchange was quenched after various times by mixing aliquots of the incubation mixture with cold 0.2 M chloroacetic acid (H_2O, pH 2) to decrease the pH to 2.5 and by decreasing the temperature to −3 °C in an ice/H_2O/ammonium sulfate bath.

Pepsin Digestion. Pepsin digestion allowed determination of the extent of deuterium incorporation into MM-CK segments during the incubation time. The deuterated sample containing 1.5 μM MM-CK was immediately proteolyzed with pepsin [in 10 mM NaH_2PO_4-AcOH/H_2O buffer (pH 2)] for 3.5 min at 0 °C (CK/pepsin ratio of 1/1) and analyzed by directly coupled HPLC and ESI-MS. Approximately 186 pmol of MM-CK was injected.

The resulting peptides were injected on a reversed-phase desalting and concentration microcolumn (Peptide Trap C-8,

3 mm × 8 mm, Michrom Bioresources) and separated on a C18 column (50 mm × 1 mm, Interchim). The HPLC column and the entire injector assembly were packed in ice to minimize H/D exchange at peptide amide linkages during analysis. An 8 min desalting step (5% mobile phase B) at a rate of 300 μL/min was used before connecting the HPLC system to the mass spectrometer. Peptides were then eluted at a rate of 50 μL/min directly into the mass spectrometer within 21 min with a 5 to 50% gradient of phase B (90% acetonitrile/0.03% TFA/H_2O) in phase A (0.03% TFA/H_2O). The column was washed with 100% phase B for 5 min after elution of the peptides. Pepsin cleavage sites are numerous and difficult to predict from sequence alone, but can be reproduced under identical digestion conditions. Therefore, all peptides were identified using MS/MS (*44*). Data were processed by centroiding an isotopic distribution corresponding to the +1, +2, or +3 charge state of each peptide.

Back-Exchange Controls. The undeuterated and totally deuterated controls were used to correct for deuterium back-exchange during analysis (*36*). The 0% reference sample was prepared by mixing a stock solution of MM-CK with buffer containing no deuterium, and the 100% deuterated reference sample was prepared by incubating the protein in 50 mM Tris-DCl/D_2O buffer (pH 2.5) at 35 °C for 3 h. These controls were also quenched and digested at the same final percentage of deuterium as the samples to correct for the gain and loss of deuterium.

Correction was done according to eq 1

$$D = \frac{m - m_{0\%}}{m_{100\%} - m_{0\%}} \times N \quad (1)$$

where D is the deuterium content of the peptide, m, $m_{0\%}$, and $m_{100\%}$ are the average molecular weights of the peptide in the sample, the undeuterated form, and the totally deuterated form, respectively, and N is the number of exchangeable peptide amide hydrogens in the protein (number of peptide bonds not involving Pro residues). The HPLC step was performed with protiated solvents, thereby removing deuterium from side chains and amino and carboxy termini that exchange much faster than amide linkages (*45*). Therefore, an increase in mass is a direct measure of the level of deuteration at peptide amide linkages.

Data Analysis. Deuterium levels were plotted versus the exchange time and fitted with a series of first-order rate expressions according to eq 2:

$$D = N - \sum a_i \exp(-k_i t) \quad (2)$$

where a_i is the number of deuterium that can be exchanged with a similar rate constant, k_i, and N is the sum of a_i (corresponding to the number of peptide amide linkages whose hydrogen exchange rate is measurable). Data were fitted to either a one- or two-exponential expression. The a_i values were rounded to the nearest integer.

Mass Spectrometry. On-line LC−MS and LC−MS/MS were performed on a quadrupole ion trap mass spectrometer (Esquire 3000+, Bruker Daltonics) operating under the following conditions: capillary voltage, 4 keV; nebulizer, 10 psi; dry gas, 8 L/min; and dry temperature, 250 °C.

Using electrospray ionization in the positive ion mode, mass spectra were acquired from *m*/*z* 200 to 2000 with averages of 25 spectra and an ICC target of 50 000.

For MS/MS analysis, mass spectra were acquired from *m*/*z* 50 to 2000 with averages of 15 spectra and an ICC target of 30 000. The threshold is 50 000; the amplitude fragmentation is 2 V between 50 and 150%, and the number of precursor ions is 3.

RESULTS

Hydrogen exchange for MM-CK in the absence or presence of substrates was assessed by incubating the protein for varying times in a deuterated buffer. After isotope exchange had been quenched, MM-CK was digested by pepsin and the masses of the resulting peptides were determined by LC−MS. This approach measured the level of deuteration at backbone amides only, because side chain deuterons quickly re-exchange with hydrogen during the liquid chromatography step. The loss of deuterium from amide linkages averaged over all peptides was 34%. Forty-seven peptides which had been identified by MS/MS covered 96% of the entire backbone. They are presented in Figure 1 together with the secondary structure. Kinetics of exchange for each peptide were satisfactorily fitted by a nonlinear least-squares method to eq 2 (see Materials and Methods), including one or two exponential terms. In our study, exchange times ranged from 5 s to 30 min while average exchange rate constants were between 0.01 and 23 min^{-1}. The amide hydrogens showing no exchange within 30 min were considered nonexchangeable ($k < 0.01$ min^{-1}). It has to be stressed that when creatine kinase was incubated with 2 mM MgADP alone, no significant protection was detected in any of the peptic peptides.

Twenty of the 47 peptides (including overlapping peptides) showed a decrease of their rate or extent of deuteration upon incubation with ADP, Mg^{2+}, NO_3^-, and creatine. Figure 2 shows the kinetics of incorporation of deuterium monitored by ESI mass spectrometry of two doubly charged peptic peptides derived from either free CK or the TSAC. Figure 2A shows that for peptide 202−224, the slow increase in deuterium content is further delayed in the liganded form, as compared with that for unliganded CK. The opposite behavior was observed for peptide 312−330 (Figure 2B) where the initial difference vanished with time.

Deuteration kinetics of representative segments are presented in Figure 3. Figure 3A shows that in peptide 54−72, which contains a large part of helix α4 (residues 52−61) and the mobile surface loop (residues 59−69), nine hydrogen amides were deuterated with an apparent rate constant of 23 min^{-1} in the unliganded CK. In the TSAC, however, only six deuterons are incorporated with the same rate constant while three are exchanged at a slower rate ($k \approx 0.2$ min^{-1}). In both cases, seven amides did not exchange or exchanged at a very slow rate. Similar results were observed for peptides 55−72, 51−72, and 54−70.

Fragment 162−186 spans a 3_{10} helix (residues 166−168), the β2 strand, which is one of the external strands of the saddle lining the active site of the enzyme, and the α8 helix (residues 180−187). Nine hydrogens exchanged rapidly ($k \approx 20$ min^{-1}) in this segment whether substrates were present or not (Figure 3B). In the free enzyme, 10 other amide hydrogens exchanged with a rate constant that was 2 orders of magnitude lower. This number was reduced to eight in the TSAC, thereby increasing the number of very slowly exchanged amide hydrogens from four to six.

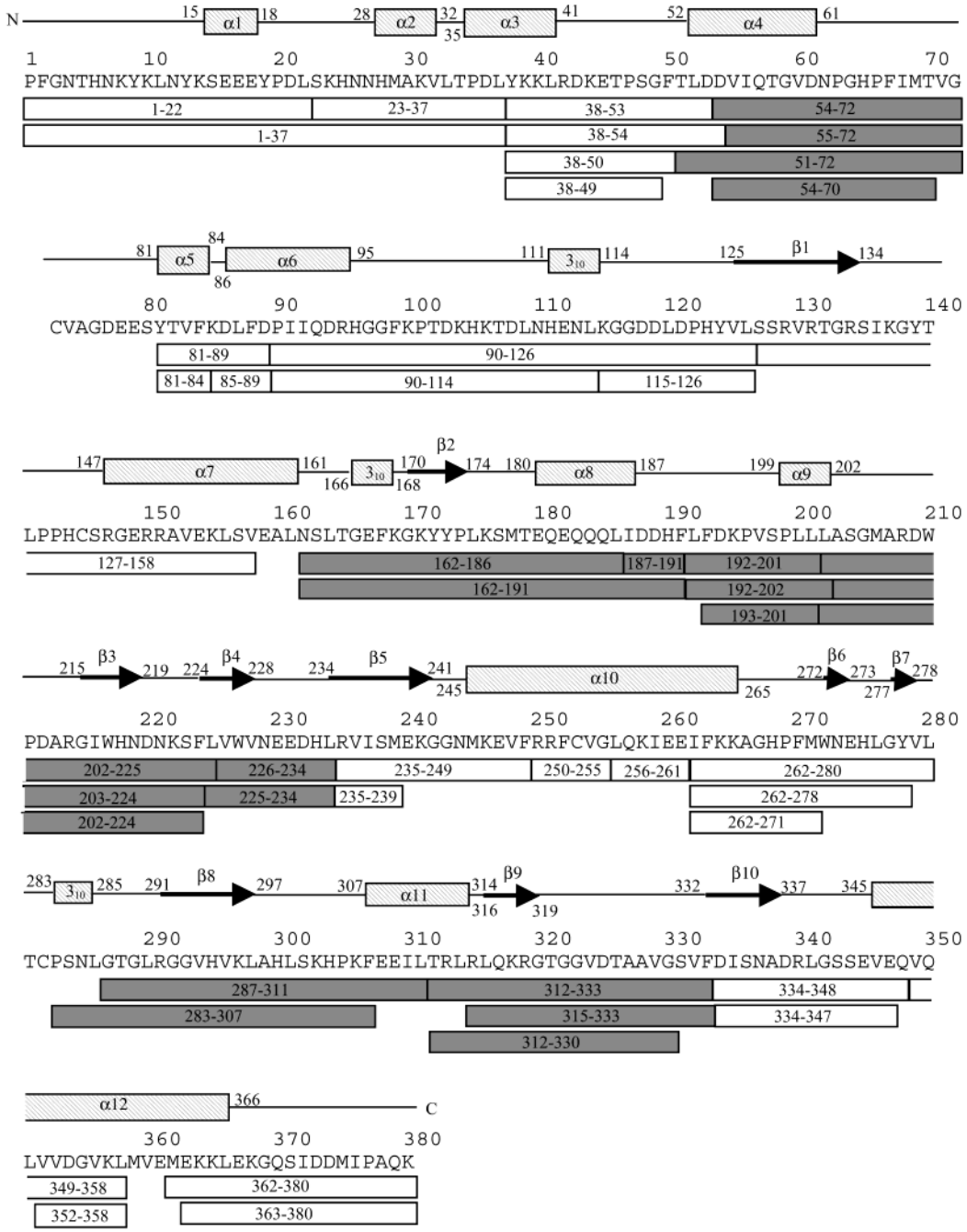

FIGURE 1: Location with respect to the rabbit MM-CK amino acid sequence of pepsin-cleaved mass-identified fragments for which deuterium incorporation was assessed. Secondary structural elements determined by X-ray crystallography (*4*) are shown above the sequence of the native protein beginning with a proline. White boxes represent the segments where the kinetics of deuteration are not altered by the presence of substrates, and gray boxes represent those where some degree of protection is afforded in the TSAC.

Peptide 193−201, which belongs to a surface region, has easily exchanged amide hydrogens: five of its six exchangeable amide hydrogens were deuterated with an apparent rate constant of 12 min^{-1}, and the last one was deuterated with a rate constant of 0.6 min^{-1} (Figure 3C). In the TSAC, the number of the most rapidly exchangeable hydrogens was reduced by three and the number of the slower ones increased by two. Thus, one hydrogen became less exchangeable. These results were confirmed by overlapping peptides 192−201 and 192−202 (not shown).

Peptide 202−224, and two overlapping peptides (203−224 and 202−225), have low levels of deuteration and similar kinetics. These peptides include the β3 strand and the beginning of the β4 strand. The three rapidly exchanged hydrogens were not affected in the TSAC (Figure 3D). Two of the more slowly exchanged protons became less exchangeable.

Weakly deuterated peptide 226−234 contains the end of the β4 strand and the turn between β4 and β5. Two hydrogens were rapidly deuterated in free CK (Figure 3E). The formation of the abortive complex completely prevented deuteration of these two exchanged hydrogens.

Another weakly deuterated peptide (residues 287−311) was partially protected in the TSAC (Figure 3F). The three rapidly exchanged hydrogens were not modified, but the

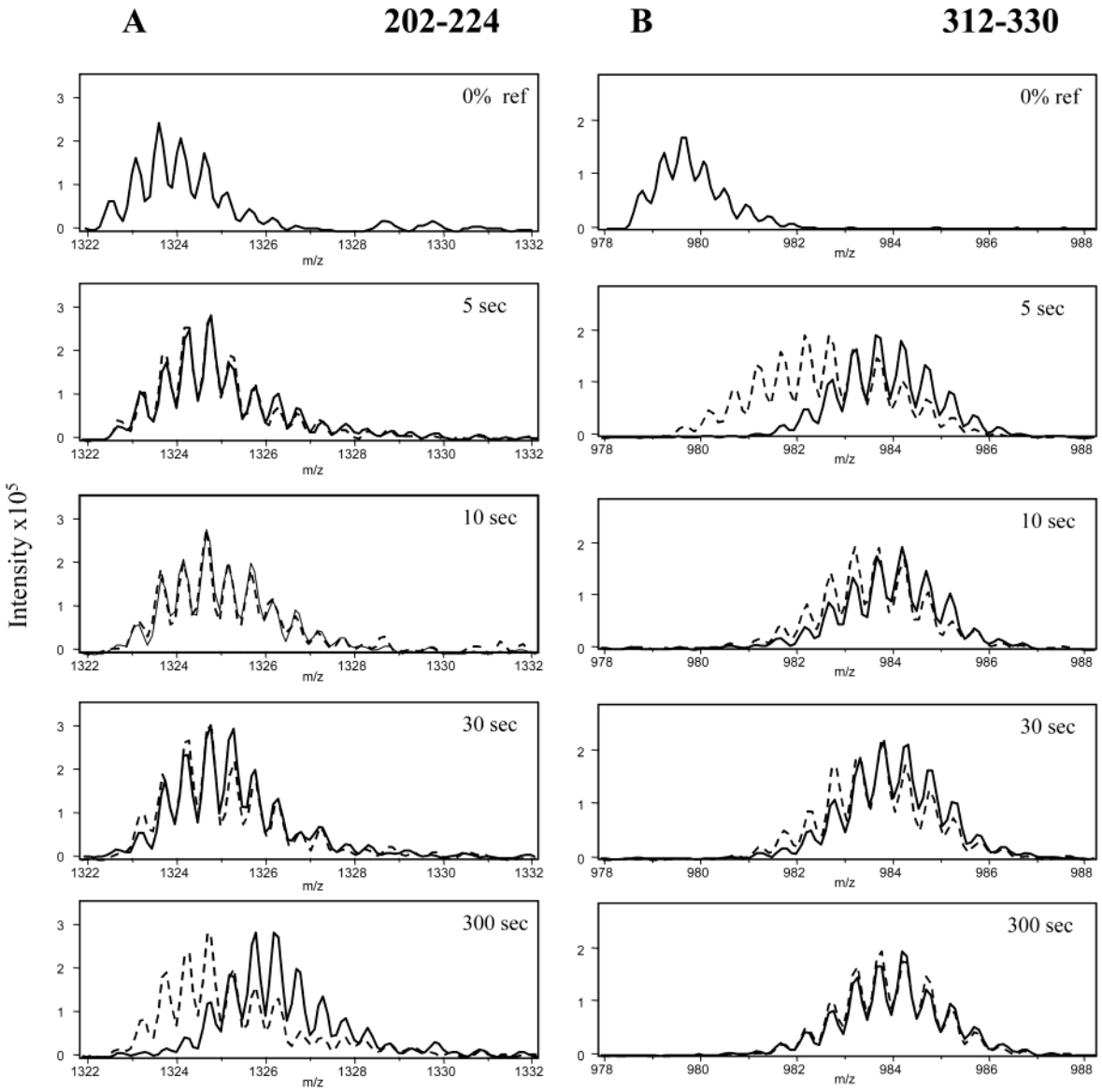

FIGURE 2: Incorporation of deuterium by two peptic fragments of CK alone (—) or incubated as the transition state analogue complex (- - -). ESI mass spectra are shown for the +2 charge state of peptide 202−224 (A) or peptide 312−330 (B). The deuteration times are indicated on the figures; 0% ref is the nondeuterated peptide.

number of more slowly deuterated NHs was reduced by three.

In peptide 315−333, a larger number of NHs were exchanged during the fast phase (Figure 3G). This fragment includes a mobile loop of which residues 322−330 were not resolved in the rabbit muscle CK crystallographic structure (*4*) and the unique proteinase K cleavage site (*24*, *25*). Two hydrogens of 15 among the rapid phase were protected in the TSAC. This increased level of protection was confirmed by the analysis of the deuteration pattern for peptides 312−330 and 312−333 (data not shown).

To summarize our results, we calculated the influence of the substrates for each peptide by dividing the increase in mass by the total number of exchangeable amide hydrogens for easier comparison between peptides of different lengths. Segments protected upon formation of the TSAC are shown on the structure of free CK (Figure 4) using a color code from yellow to red, which reflects the changes in deuterium levels. Most of them are located in or at the entrance of the active site.

DISCUSSION

Structure−function relationships in CK have been the subject of numerous studies. Kinetics of rabbit muscle cytoplasmic CK follow a random-order, rapid equilibrium mechanism (*46*, *47*) where binding of a first substrate improves the binding of the second one. Milner-White and Watts (*16*) were the first to document the formation of a quaternary CK−MgADP−anion−creatine complex in the presence of some monovalent anions, the most efficient of which was the nitrate ion.

The conformation of this dead-end complex was believed to be very similar to that of the reactive transition state on the catalytic pathway (*48*). It was supposed that the NO_3^- anion occupied the position of the transferable phosphate during the transition state of the enzymatic reaction, and this was later confirmed by the crystal structures of the TSAC of arginine kinase and *T. californica* creatine kinase (*17*, *18*). The stability of this complex is very high and the affinity of each of its components can be measured by fluorescence

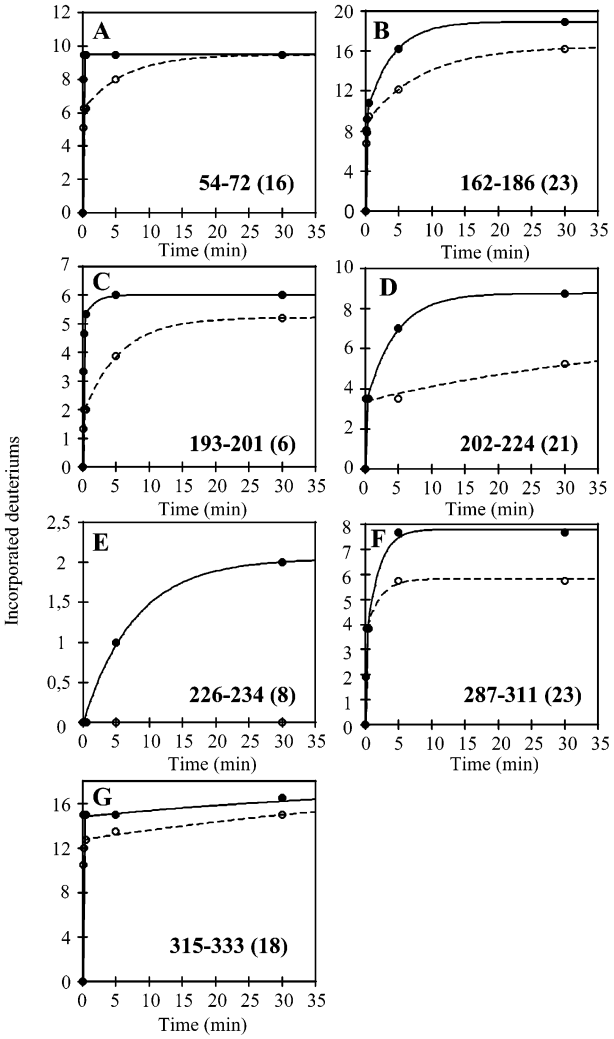

FIGURE 3: Deuterium exchange-in curves for seven fragments produced by pepsin digestion of CK alone (●) or incubated as the transition state analogue complex (○). The number of backbone exchangeable amide hydrogens is indicated in parentheses. The data in the panels are fitted to eq 2 with two exponential terms. Peptide 54−72 in unliganded CK and peptide 226−234 in the TSAC were fitted to an equation with one exponential term. The slowest exchanging protons could not be detected on the time scale of the experiments.

quenching (*49*). In this section, we discuss our H/D exchange results with the free MM-CK and the TSAC in view of the available structural information for the free rabbit muscle enzyme (*4*) and for the transition state of the similar *T. californica* CK (*18*).

Among the seven regions that we have found protected in the TSAC, two belong to the highly flexible loops, which had been hypothesized to move upon substrate fixation (residues 59−69 and 320−330). Indeed, as shown by the crystallographic structure of the TSAC of CK from *T. californica*, these two loops moved toward each other in conjunction with the binding of the substrates, and His65 interacts with Asp325 to give a closed conformation of the active site from where water molecules are excluded (*18*).

As expected for a very accessible segment, the equivalent of nine of the sixteen exchangeable amide hydrogens in peptide 54−72 are rapidly deuterated. However, in the TSAC, the rate of exchange of three of them is reduced. These three NHs may well be located after Ile68 which,

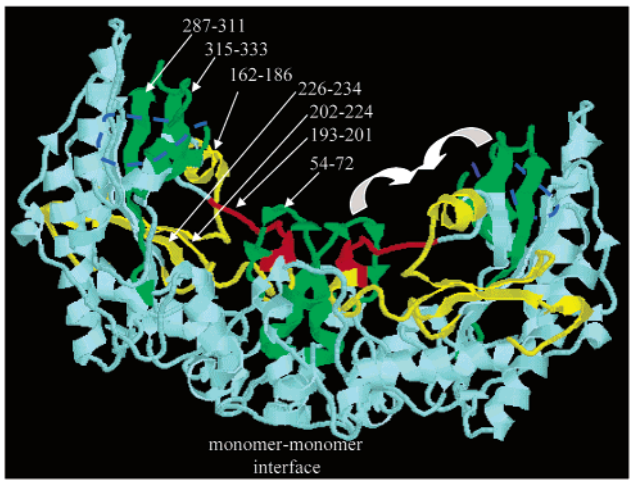

FIGURE 4: Influence of ADP−Mg^{2+}−NO^{3-}−creatine binding on the conformation of creatine kinase as reported by H/D exchange mapping of peptic peptides. For visualization purposes, the regions of the structure of the noncomplexed dimeric MM-CK, where a decreased level of deuterium incorporation was observed, are color coded. After a deuteration period of 5 min, the green segments exhibit a decrease in the level of deuterium incorporation from 0 to 10%, the yellow ones exhibit a decrease from 11 to 20%, and the red one exhibits a decrease from 21 to 40%. The position of residues 322−330, which is not modeled in the crystallographic structure of Rao *et al*. (*4*), is drawn as a blue dashed line as depicted for the open conformation of *T. californica* CK. Two arrows indicate the closing movement of the two flexible loops upon formation of the enzyme−substrate complex (*18*).

together with Val324, participates in the formation of a hydrophobic pocket for the creatine methyl group (*18*), in which access of D_2O to the amide hydrogens will be restricted. Furthermore, it has been demonstrated that the backbone NH of Val71 is hydrogen bonded to the carboxylate group of creatine, which may slow its deuteration. Helix α4 is located at the interface between monomers. Thus, its NHs may be included in the seven nondeuterated amides that were not affected in the TSAC.

Fifteen of the 18 amide hydrogens of peptide 315−333, which probe the other very mobile loop on the other side of the active site, were also rapidly exchanged. The three slowly exchanged hydrogens are likely to be located in strand *β*9, which constitutes the N-terminal end of this probe. Two hydrogens become very slowly exchangeable in the TSAC. As previously stated, this loop undergoes a large movement toward the active site so that Asp325 interacts with His65 of the N-terminal loop (*18*). This movement allows several residues to make contact with the substrates: Arg319 with nitrate and both phosphates of ADP and the Gly322 NH and that of Val324 with the ribose moiety and the α-phosphate of ADP, respectively. The two latter hydrogens could then be those which became protected upon formation of the TSAC.

The deuteration of two other highly exchangeable probes was affected in the TSAC. In peptide 162−186, nine of 23 exchangeable amides were rapidly deuterated because they were not protected, whereas two of the 10 slowly deuterated ones were further protected and became less exchangeable. There is no obvious reason for this increased level of protection since this segment is located relatively far from the active site. However, close examination of the structural data reveals the proximity of His190, located between the

end of this probe and the beginning of the next one (residues 193−201), which interacts with the ribose 2′-hydroxyl in the TSAC. This slight protection may result from the location of this peptide in a region in which the conformation is altered by the rotation of the domains upon substrate binding.

The deuteration of the other highly exchangeable probe (residues 193−201) is strongly modified in the TSAC since the rate of deuteration of two of its six exchangeable amide hydrogens was reduced and that of a third one was even more reduced. This probe contains Lys195, which is an interface residue between monomers (*4*, *8*). However, in the open conformation, this peptide can be accessible from within the active site, but is protected against the solvent after closing of the site in the substrate-bound conformation. This is a reasonable explanation for the large degree of protection of this peptide in the TSAC.

Probe 202−224 is less than 50% deuterated in unliganded CK. Indeed, it comprises strand β3 and part of strand β4, which belong to the eight-stranded antiparallel β-sheet lining the active site. This saddle-shaped β-sheet is part of the hydrophobic core of the protein, which plays a major role in the structure of this active site. It contains Trp217 which, among the tryptophan residues, is the weaker contributor to CK fluorescence (*14*). This fragment also comprises Trp210 which, along with Leu202, Ala207, Arg208, Asp209, and Asp212, belongs to a large interface segment between monomers which consequently will have limited access to the solvent (*4*, *8*). The three rapidly exchanged amides, which were not affected by the formation of the TSAC, may be located between Asp212 and strand β3 or in the surface segment between strands β3 and β4. The protection of two slowly exchangeable hydrogens cannot be explained by a direct interaction with the substrates but by a possible conformational or positional change in this peptide.

The next peptide (residues 226−234) is also part of the large β-sheet of the C-terminal domain, which explains its weak deuteration. It contains Trp227, which is crucial for catalytic activity; this residue is poorly accessible to the solvent, and it is the strongest contributor to total fluorescence in MM-CK, as well as in mitochondrial CK (*14*, *50*). In the TSAC, Glu231 interacts with the guanidinium side chain of creatine, and the nearby residue in the primary structure, Arg235, interacts with the β-phosphate of ADP and NO_3^-. Thus, this fragment is a part of the active site, which is a dynamic structure giving selective access to the substrates, but not to the bulk solvent. This dynamic behavior may explain the suppression of deuteration of the two exchangeable protons in the TSAC.

The number of rapidly exchangeable hydrogens in probe 287−311 is unmodified in the TSAC, suggesting that these three hydrogens may be located in the accessible turn between strand β8 and helix α11. In this fragment, two residues make contact with the ligands: Arg291 with the β-phosphate of ADP and His295, which stacks over the adenine moiety. Thus, this fragment is also part of the active site, which may explain the protection of three slowly exchangeable NHs as a consequence of their diminished solvent accessibility.

In summary, as illustrated in Figure 4, we have found that the exchange rates of most of CK peptides are not affected in the TSAC except for seven areas that are protected to some degree against H/D exchange as a result of an induced fit. Four of them can be considered part of the substrate binding sites (peptides 54−72, 315−333, 226−234, and 287−311) by analogy with the three-dimensional structure of the TSAC of *T. californica* CK (*18*). The other three (peptides 162−186, 193−201, and 202−224) are not directly involved in the binding of substrates. Such structural changes remote from the active site were also found in an isomeroreductase (*40*) and were interpreted as long-range effects of the ligand binding process. Very recently, a direct comparison between both open and closed forms of arginine kinase from *Limulus polyphemus* has revealed substrate-induced domain motion (*51*). Indeed, the three last mentioned peptides correspond to dynamic domain 2 of arginine kinase which undergoes a hinge rotation upon formation of the TSAC. The lower rates of exchange could be interpreted on the basis of new hydrogen bonding, lower solvent accessibility, reduced residue mobility, or combinations thereof. In CK, no probe was found to exhibit an increase in the level of deuteration upon substrate binding as was observed in the regulatory subunit of protein kinase A (*52*).

Our results strengthen the information about the active state of CK recently provided by the determination of the three-dimensional structure of the *T. californica* transition state analogue complex (*18*) and by that of the open and closed states of arginine kinase (*51*). However, these results do not provide evidence for the alternating active subunit mechanism suggested by Lahiri *et al*. (*18*) on the basis of a crystallographic asymmetric unit comprising one monomer in the CK-ADP state and one in the TSAC state. Since the affinity of the substrates for the enzyme in the TSAC is very high ($K_d = 3 \times 10^{-10}$ M^3) (*49*), nearly all the binding sites will be saturated. Under these conditions, according to Lahiri *et al*., half of the subunits would have to be in an open conformation (MgADP bound) with the corresponding level of deuteration (exchange obtained with MgADP is indistinguishable from that obtained without the substrate). It is very likely that the kinetics of association and dissociation are fast on the labeling step time scale, thus eventually reducing the level of protection afforded in the closed conformation. From Figure 2A, it is obvious that even for long exchange reactions, the TSAC is more than half-protected. This holds true for results in Figure 2B and for other peptides. These new data strongly suggest that, in solution, both subunits within a dimer can bind the substrates.

Our data contribute to the identification and localization of enzyme areas that experience conformational changes upon formation of the transition state analogue complex. These areas could be implicated in the proper alignment of CK substrates against each other. Indeed, as suggested by Stroud (*53*), multisubstrate enzymes such as CK may act by "convening" substrate interactions in correct orientations.

ACKNOWLEDGMENT

We thank Prof. David L. Smith for helpful advice and discussions.

REFERENCES

1. Wallimann, T., Wyss, M., Brdiczka, D., Nicolay, K., and Eppenberger, H. M. (1992) Intracellular compartmentation, structure and function of creatine kinase isoenzymes in tissues with high and fluctuating energy demands: The phosphocreatine circuit for cellular energy homeostasis, *Biochem. J. 281*, 21−40.

2. Fritz-Wolf, K., Schnyder, T., Wallimann, T., and Kabsch, W. (1996) Structure of mitochondrial creatine kinase, *Nature 381*, 341−345.
3. Kabsch, W., and Fritz-Wolf, K. (1997) Mitochondrial creatine kinase: A square protein, *Curr. Opin. Struct. Biol. 7*, 811−818.
4. Rao, J. K. M., Bujacz, G., and Wlodawer, A. (1998) Crystal structure of rabbit muscle creatine kinase, *FEBS Lett. 439*, 133−137.
5. Eder, M., Schlattner, U., Becker, A., Wallimann, T., Kabsch, W., and Fritz-Wolf, K. (1999) Crystal structure of brain-type creatine kinase at 1.41 Å resolution, *Protein Sci. 8*, 2258−2269.
6. Eder, M., Fritz-Wolf, K., Kabsch, W., Wallimann, T., and Schlattner, U. (2000) Crystal structure of human ubiquitous mitochondrial creatine kinase, *Proteins 39*, 216−225.
7. Shen, Y. Q., Tang, L., Zhou, H. M., and Lin, Z. J. (2001) Structure of human muscle creatine kinase, *Acta Crystallogr. D57*, 1196−1200.
8. Webb, T. I., and Morris G. E. (2001) Structure of an intermediate in the unfolding of creatine kinase, *Proteins 42*, 269−278.
9. Roustan, C., Kassab, R., Pradel, L. A., and Van Thoai, N. (1968) Interaction des ATP: guanidine phosphotransférases avec leurs substrats, étudiée par spectrophotométrie différentielle, *Biochim. Biophys. Acta 167*, 326−338.
10. Roustan, C., Pradel, L. A., Kassab, R., Fattoum, A., and Thoai, N. V. (1970) Spectrophotometric investigations of the interaction of native and chemically modified ATP: guanidinophosphotransferases with their substrates, *Biochim. Biophys. Acta 206*, 369−379.
11. Price, N. C. (1972) The interaction of nucleotides with kinases, monitored by changes in protein fluorescence, *FEBS Lett. 24*, 21−23.
12. Vasak, M., Nagayama, K., Wüthrich, K., Mertens, M. L., and Kägi, H. R. (1979) Creatine kinase. Nuclear magnetic resonance and fluorescence evidence for interaction of adenosine 5′-diphosphate with aromatic residue(s), *Biochemistry 18*, 5050−5055.
13. Messmer, C. H., and Kägi, H. R. (1985) Tryptophan residues of creatine kinase: a fluorescence study, *Biochemistry 24*, 7172−7178.
14. Gross, M., Furter-Graves, E. M., Wallimann, T., Eppenberger, H. M., and Furter, R. (1994) The tryptophan residues of mitochondrial creatine kinase: Roles of Trp-223, Trp-206, and Trp-264 in active-site and quaternary structure formation, *Protein Sci. 3*, 1058−1068.
15. Clottes, E., and Vial, C. (1996) Discrimination between the four tryptophan residues of MM-creatine kinase on the basis of the effect of N-bromosuccinimide on activity and spectral properties, *Arch. Biochem. Biophys. 329*, 97−103.
16. Milner-White, E. J., and Watts, D. C. (1971) Inhibition of adenosine 5′-triphosphate-creatine phosphotransferase by substrate-anion complexes, *Biochem. J. 122*, 727−740.
17. Zhou, G., Somasundaram, T., Blanc, E., Parthasarathy, G., Ellington, W. R., and Chapman, M. S. (1998) Transition state structure of arginine kinase: implications for catalysis of bimolecular reactions, *Proc. Natl. Acad. Sci. U.S.A. 95*, 8449−8454.
18. Lahiri, S. D., Wang, P. F., Babbitt, P. C., McLeish, M. J., Kenyon, G. L., and Allen, K. N. (2002) The 2.1 Å structure of *Torpedo californica* creatine kinase complexed with the ADP−Mg^{2+}−NO_3^-−creatine transition-state analogue complex, *Biochemistry 41*, 13861−13867.
19. Suzuki, T., Kawasaki, Y., Furukohri, T., and Ellington, W. R. (1997) Evolution of phosphagen kinase. VI. Isolation, characterization and cDNA-derived amino acid sequence of lombricine kinase from the earthworm *Eisenia foetida*, and identification of a possible candidate for the guanidine substrate recognition site, *Biochim. Biophys. Acta 1343*, 152−159.
20. Reed, G. H., and Cohn, M. (1972) Structural changes induced by substrates and anions at the active site of creatine kinase. Electron paramagnetic resonance and nuclear magnetic relaxation rate studies of the manganous complexes, *J. Biol. Chem. 247*, 3073−3081.
21. Williamson, J., Greene, J., Cherif, S., and Milner-White, E. J. (1977) Heterogeneity of rabbit muscle creatine kinase and limited proteolysis by proteinase K, *Biochem. J. 167*, 731−737.
22. Price, N. C., Murray, S., and Milner-White, E. J. (1981) The effect of limited proteolysis on rabbit muscle creatine kinase, *Biochem. J. 199*, 239−244.
23. Lebherz, H. G., Burke, T., Shackelford, J. E., Strickler, J. E., and Wilson, K. J. (1986) Specific proteolytic modification of creatine kinase isoenzymes. Implication of C-terminal involvement in enzymic activity but not in subunit-subunit recognition, *Biochem. J. 233*, 51−56.
24. Wyss, M., James, P., Schlegel, J., and Wallimann, T. (1993) Limited proteolysis of creatine kinase: Implications for 3-dimensional structure and for conformational substates, *Biochemistry 32*, 10727−10735.
25. Leydier, C., Andersen, J. S., Couthon, F., Forest, E., Marcillat, O., Denoroy, L., Vial, C., and Clottes, E. (1997) Proteinase K processing of rabbit muscle creatine kinase, *J. Protein Chem. 16*, 67−74.
26. Price, N., and Hunter, M. G. (1976) Non-identical behaviour of the subunits of rabbit muscle creatine kinase, *Biochim. Biophys. Acta 445*, 364−376.
27. Rosevear, P. R., Desmeules, P., Kenyon, G. L., and Mildvan, A. S. (1981) Nuclear magnetic resonance studies of the role of histidine residues at the active site of rabbit muscle creatine kinase, *Biochemistry 20*, 6155−6164.
28. Leydier, C., Clottes, E., Couthon, F., Marcillat, O., and Vial, C. (1997) Involvement of a tyrosine residue in the ADP binding site of creatine kinase. A second-derivative UV-spectroscopy study, *Biochem. Mol. Biol. Int. 41*, 777−784.
29. Borders, C. L., and Riordan, J. F. (1975) An essential arginyl residue at the nucleotide binding site of creatine kinase, *Biochemistry 14*, 4699−4704.
30. Raimbault, C., Buchet, R., and Vial, C. (1996) Changes of creatine kinase secondary structure induced by the release of nucleotides from caged compounds: An infrared difference-spectroscopy study, *Eur. J. Biochem. 240*, 134−142.
31. Raimbault, C., Clottes, E., Leydier, C., Vial, C., and Buchet, R. (1997) ADP-binding and ATP-binding sites in native and proteinase-K-digested creative kinase, probed by reaction-induced difference infrared spectroscopy, *Eur. J. Biochem. 247*, 1197−1208.
32. Granjon, T., Vacheron, M. J., Vial, C., and Buchet, R. (2001) Structural changes of mitochondrial creatine kinase upon binding of ADP, ATP or Pi, observed by reaction-induced infrared difference spectra, *Biochemistry 40*, 2988−2994.
33. Forstner, M., Kriechbaum, M., Laggner, P., and Wallimann, T. (1998) Structural changes of creatine kinase upon substrate binding, *Biophys. J. 75*, 1016−1023.
34. Englander, S. W., and Kallenbach, N. R. (1984) Hydrogen exchange and structural dynamics of proteins and nucleic acids, *Q. Rev. Biophys. 16*, 521−655.
35. Roder, H., Wagner, G., and Wüthrich, K. (1985) Individual amide proton exchange rates in thermally unfolded basic pancreatic trypsin inhibitor, *Biochemistry 24*, 7407−7411.
36. Zhang, Z., and Smith, D. L. (1993) Determination of amide hydrogen exchange by mass spectrometry: a new tool for protein structure elucidation, *Protein Sci. 2*, 522−531.
37. Wang, F., Blanchard, J. S., and Tang, X. J. (1997) Hydrogen exchange/electrospray ionization mass spectrometry studies of substrate and inhibitor binding and conformational changes of *Escherichia coli* dihydrodipicolinate reductase, *Biochemistry 36*, 3755−3759.
38. Wang, F., Scapin, G., Blanchard, J. S., and Angeletti, R. H. (1998) Substrate binding and conformational changes of *Clostridium glutamicum* diaminopimelate dehydrogenase revealed by hydrogen/deuterium exchange and electrospray mass spectrometry, *Protein Sci. 7*, 293−299.
39. Wang, F., Li, W., Emmett, M. R., Hendrickson, C. L., Marshall, A. G., Zhang, Y., Wu, L., and Zhang, Z. Y. (1998) Conformational and dynamic changes of *Yersinia* protein tyrosine phosphatase induced by ligand binding and active site mutation and revealed by H/D exchange and electrospray ionization Fourier transform ion cyclotron resonance mass spectrometry, *Biochemistry 37*, 15289−15299.
40. Halgand, F., Dumas, R., Biou, V., Andrieu, J. P., Thomazeau, K., Gagnon, J., Douce, R., and Forest, E. (1999) Characterization of the conformational changes of acetohydroxy acid isomeroreductase induced by the binding of Mg^{2+} ions, NADPH, and a competitive inhibitor, *Biochemistry 38*, 6025−6034.
41. Andersen, M. D., Shaffer, J., Jennings, P. A., and Adams, J. A. (2001) Structural characterization of protein kinase A as a function of nucleotide binding, *J. Biol. Chem. 276*, 14204−14211.
42. Resing, K. A., and Ahn, N. G. (1998) Deuterium exchange mass spectrometry as a probe of protein kinase activation. Analysis of wild-type and constitutively active mutants of MAP kinase kinase-1, *Biochemistry 37*, 463−475.

43. Connelly, G. P., Bai, Y., Jeng, M. F., and Englander, S. W. (1993) Isotope effects in peptide group hydrogen exchange, *Proteins 17*, 87−92.
44. Biemann, K. (1992) Mass spectrometry of peptides and proteins, *Annu. Rev. Biochem. 61*, 977−1010.
45. Bai, Y., Milne, J. S., Mayne, L., and Englander, S. W. (1993) Primary structure effects on peptide group hydrogen exchange, *Proteins 17*, 75−86.
46. Morrison, J. F., and James, E. (1965) The mechanism of the reaction catalysed by adenosine triphosphate-creatine phosphotransferase, *Biochem. J. 97*, 37−52.
47. Maggio, E. T., Kenyon, G. L., Markham, G. D., and Reed, G. H. (1977) Properties of a CH_3S-blocked creatine kinase with altered catalytic activity, *J. Biol. Chem. 252*, 1202−1207.
48. Travers, F., and Barman, T. E. (1980) Cryoenzymic studies on the transition-state analog complex creatine kinase ADPMg nitrate creatine, *Eur. J. Biochem. 110*, 405−412.
49. Borders, C. L., Jr., Snider, M. J., Wolfenden, R., and Edmiston, P. L. (2002) Determination of the affinity of each component of a composite quaternary transition-state analogue complex of creatine kinase, *Biochemistry 41*, 6995−7000.
50. Darmochod, S., Marcillat, O., and Vial, C. (1996) unpublished results.
51. Yousef, M. S., Clark, S. A., Pruett, P. K., Somasundaram, T., Ellington, W. R., and Chapman, M. S. (2003) Induced-fit in guanidino kinases: comparison of substrate-free and transition state analog structures of arginine kinase, *Protein Sci. 12*, 103−111.
52. Anand, G. S., Hughes, C. A., Jones, J. M., Taylor, S. S., and Komives, E. A. (2002) Amide $H/^2H$ exchange reveals communication between the cAMP and catalytic subunit-binding sites in the R′α subunit of protein kinase A, *J. Mol. Biol. 323*, 377−386.
53. Stroud, R. M. (1996) Balancing ATP in the cell, *Nat. Struct. Biol. 3*, 567−569.

BI035208M